Free-swimming swordfish, *Xiphias gladius*, alter the rate of whole body heat transfer: morphological and physiological specializations for thermoregulation

Ashley Stoehr[1],*, Joshua St. Martin[1], Scott Aalbers[2], Chugey Sepulveda[2], and Diego Bernal[1]

[1]Department of Biology, University of Massachusetts Dartmouth, 285 Old Westport Road, Dartmouth, MA 02747, USA
[2]Pfleger Institute of Environmental Research, PIER, 210 S Coast Highway F, Oceanside, CA 92054, USA

*Corresponding author: tel: +508 999 8208; fax: +508 999 8217; e-mail: astoehr@umassd.edu

Stoehr, A., St. Martin, J., Aalbers, S., Sepulveda, C., and Bernal, D. Free-swimming swordfish, *Xiphias gladius*, alter the rate of whole body heat transfer: morphological and physiological specializations for thermoregulation. – ICES Journal of Marine Science, doi:10.1093/icesjms/fsx163.

Swordfish (*Xiphias gladius*) are large, highly-migratory pelagic, fishes that make diel, vertical excursions from the warm, surface layer (e.g. 18–24 °C) to the cold waters (~8 °C) below the thermocline (300–600 m). They possess anatomical traits [e.g. medial red muscle (RM) position and an associated vascular rete] that could enable metabolic heat-retention and result in RM temperature elevation above ambient, or RM endothermy. We herein provide: (i) expanded anatomical descriptions of the RM-associated vasculature (i.e. central rete and lateral blood vessels), (ii) new measurements of *in vivo* temperature, and (iii) heat transfer models to assess the capacities for RM endothermy and physiological thermoregulation during vertical movements. Despite the presence of a medial RM and two associated blood-flow pathways (one of which forms a rete), swordfish exhibited a limited capacity for RM endothermy, with muscle temperatures approaching ambient during prolonged periods above or below the thermocline. Our heat transfer models suggest, however, that swordfish may control rates of heat loss or gain during vertical movements, possibly by altering the route of blood flow supplying the RM. Such physiological thermoregulation likely contributes to the ability of swordfish to capitalize on food resources below the thermocline, which are out of range for most other active, pelagic fishes.

Keywords: endothermy, high performance fishes, red muscle, thermoregulation, vascular anatomy, vertical movement.

Introduction

Swordfish (*Xiphias gladius*) are large, active, pelagic teleost fishes that are exploited by large-scale commercial fisheries across all ocean basins (50°N–50°S; Ward *et al.*, 2000) and make seasonal migrations from the tropics to foraging grounds in temperate and sub-polar waters (Abascal *et al.*, 2010). They are also capable of diel, vertical movements from the warm, upper mixed layer (~18–24 °C) to cold waters (~8 °C) well below the thermocline (300–600 m), where they feed on prey associated with the deep-scattering layer (Carey and Robinson, 1981; Carey and Gibson, 1987; Carey, 1990; Takahashi *et al.*, 2003; Sepulveda *et al.*, 2010; Dewar *et al.*, 2011).

Initial work on the extensive vertical mobility of swordfish attributed their extreme thermal tolerance to the presence of a brain and eye heating complex, which is derived from a modified ocular muscle (i.e. superior rectus) and elevates the temperature of the eyes and brain above ambient (Carey, 1982; Block, 1986; Fritsches *et al.*, 2005). Warming of the cranial region was proposed to buffer the central nervous system from rapid temperature changes, and allow swordfish to tolerate prolonged exposure to cold water at depth (Carey, 1982; Block, 1986; Fritsches *et al.*, 2005). Although this hypothesis is well supported, questions remain as to how swordfish, which are obligate ram ventilators (Wegner *et al.*, 2010), cope with the potentially detrimental

effects that large and rapid temperature changes impose on locomotor muscle function (Bennett, 1984; Block and Finnerty, 1994). The thermal tolerance of the swimming muscles may directly impact the ability of swordfish to exploit a range of environments on a seasonal (i.e. movements from tropical to temperate areas) or daily basis (i.e. vertical movements from the surface to well below the thermocline) (Brill and Lutcavage, 2001).

In general, fish locomotion is powered by two discretely segregated fibre types, glycolytic, white muscle (WM) that is used during short-duration burst swimming, and aerobic, red muscle (RM) that powers sustained swimming (Johnston, 1981). Studies of pelagic fishes that have the capacity to elevate RM temperature above water temperature (i.e. RM endothermy) have shown a correlation between RM temperatures and sustained swimming capacity (Block and Finnerty, 1994; Bernal et al., 2001; Dickson and Graham, 2004). Field and laboratory investigations on the aerobic capacity and locomotor performance of these fishes suggest that RM endothermy enhances sustained swimming performance (e.g. greater swimming speeds, larger maximum annual migration ranges) by allowing for an RM temperature that is elevated above and fluctuates less then water temperature, a scenario unlike that present in sympatric ectothermic fishes (Block and Finnerty, 1994; Dickson, 1995, 1996; Bernal et al., 2001; Dickson and Graham, 2004; Watanabe et al., 2015).

RM endothermy in fishes is made possible by a suite of morphological and physiological specializations that permit metabolic heat retention (Carey et al., 1971; Block and Finnerty, 1994; Brill, 1994). More specifically, the RM is positioned medially, or closer to the vertebrae, and is served by a complex network of arteries and veins, which form countercurrent heat-exchanging retia (Carey and Teal, 1966; Carey et al., 1971; Bone and Chubb, 1983; Graham et al., 1983; Block and Finnerty, 1994; Dewar et al., 1994b; Patterson et al., 2011). Interestingly, swordfish are the only teleost species, other than the scombroid fishes, to exhibit a medially positioned RM that is served by a putative vascular rete; but, it is unclear to what degree these specializations function to control RM temperatures, especially during exposure to large and rapid changes in ambient conditions (Carey, 1990; Figure 1a).

Previous work using acoustic telemetry and archival (i.e. data recording) tagging has documented the sizeable vertical movement patterns of free-swimming swordfish, showing their extensive capacity to undergo prolonged descents below the thermocline (Carey and Robinson, 1981; Takahashi et al., 2003; Sepulveda et al., 2010; Dewar et al., 2011). Records of deep body temperature (presumably that of the RM) were not, however, able to confirm a high capacity for RM endothermy (Carey and Gibson, 1987; Carey, 1990). Rather, the data suggested that body temperature fluctuated widely during daily vertical movements, a scenario contrasting that described for fishes with RM endothermy (Carey et al., 1971, 1982; Holland and Sibert, 1994). Nevertheless, the manner in which body temperature changed throughout the vertical movement cycle suggested differential heating and cooling rates (Carey, 1990). This implies that swordfish have the ability to modulate heat transfer rates, or to physiologically thermoregulate, perhaps by changing the rates or routes of blood flow to the RM (Carey, 1990; Brill et al., 1994).

There are, to date, no detailed anatomical descriptions of the RM-associated vasculature and only limited field-based data that can be used to assess the capacities for RM endothermy or physiological thermoregulation in swordfish. Our objectives were, therefore, to: (i) provide a more detailed anatomical description of the vascular blood supply to the RM; (ii) record in vivo temperatures (i.e. RM) of free-swimming swordfish, and (iii) develop thermodynamic models describing heat transfer between the RM and the environment during diel vertical movements. Taken together, our data provide insight into the ecology of swordfish; and we propose hypotheses on how this wide-ranging species has (unlike other large, predatory, pelagic fishes) evolved the capacity to tolerate extreme temperature fluctuations, the cornerstone of its ability to exploit extensive geographic areas and depths.

Methods

All capture and handling procedures followed guidelines approved by the University of Massachusetts animal care protocol no. 13-06 and California Department of Fish and Wildlife Scientific Collection permit no. SC-2471.

Investigations of RM-associated vasculature anatomy

Swordfish ($n = 4$; 90–130 cm lower jaw-fork length, LJFL were captured by pelagic long-line (F/V Eagle Eye II and R/V Oscar Sette) or deep-set buoy gear (R/V Malolo; Sepulveda et al., 2014). Specimens were transported back to the laboratory and dissected to determine the origin and trajectory of the major arteries between the gills and the RM, and the major veins returning from the RM to the heart. We exposed and removed the viscera, as well as any connective tissue and bone, to expose the heart, efferent branchial arteries (EBAs), dorsal aorta (DA), and post-cardinal vein (PCV) using an incision from the pectoral girdle to the cloaca. We exposed the lateral artery (LA), first described by Carey (1990), via parasagittal cuts (∼5 mm thick) that removed the overlying skin and superficial WM. Systemic arteries were identified as any blood vessel originating from the EBA or its associated branches; this included the DA and LA (Carey, 1990; Dickson, 1994). Veins were similarly identified as any blood vessel that terminated at the pericardial cavity or an associated sinus; this included the PCV and its supplying branches. We traced all major blood vessels posteriorly from the heart (e.g. DA and PCV) or gills (e.g. LA), as well as any blood vessels running towards and through the RM until they either became indistinguishable from the surrounding tissue or joined another identifiable vessel.

Tissue sample blocks (∼10 × 10 × 10 mm) extending inwards from the LA towards the vertebrae were removed and sent to a commercial laboratory (Mass Histology; Worcester, MA) where they were dehydrated in a graded ethanol series, cleared in xylene, embedded in paraffin wax, cut with a microtome (∼5 μm thick), and stained with Masson's trichrome or H&E to allow visualization of the lumen in any blood vessels travelling through the RM, from the lateral circulation towards the central circulation (i.e. DA and PCV complex). We distinguished sectioned arteries and veins by both the relative size of the tunica media (i.e. the layer comprised of smooth muscle cells intermingled with elastic fibres is larger in arteries) in the vascular wall and the overall shape (arteries tend to remain circular in histological preparations) (Young et al., 2000).

Analysis of ambient and body temperature

Swordfish ($n = 6$; 220–250 cm LJFL, ∼90–140 kg) were tagged in the Southern California Bight at ∼33°00′N, 117°50′W. The electronics package consisted of a Lotek (Newfoundland, CA) model 1410 archival tag affixed to a Wildlife Computers (Redmond,

WA, USA) MK10 pop-off satellite archival tag (PSAT). The Lotek tag had a 10 cm external thermistor lead that was inserted into an 8 cm long 3 mm diameter section of inert tubing and attached to the PSAT plastic, umbrella anchor (Domeier *et al.*, 2005). Swordfish were tagged using a modified harpoon from the bow pulpit or using a smaller hand-held tagging stick from the side of the boat following capture by deep-set buoy gear. The position of the plastic umbrella anchor was adjusted on the harpoon or tagging stick such that the thermistor tip penetrated the deep tissue at a depth estimated as proximal to the RM (e.g. for a body mass between 90 and 140 kg the RM is ∼10 cm under skin). Tags were programmed to record ambient temperature (T_a, °C), RM temperature (T_{RM}, °C), and depth once every minute. The PSATs were programmed to detach four to 6 days after deployment, and were recovered using a Gonio 400 (SERPE-IESM, Guidel, France) signal direction finder. The T_a, T_{RM}, and depth data were downloaded from the tags and imported into ACCESS database (Microsoft Office, 2003, Seattle, WA, USA).

RM endothermy

We quantified the capacity for RM endothermy by measuring the temperature excess (T_x) of the RM (where $T_x = T_{RM} - T_a$) during steady state conditions (i.e. periods of at least 10 min when changes in T_{RM} and T_a were < 0.1 °C, as in Neill *et al.*, 1976).

Physiological thermoregulation

We quantified the capacity for physiological thermoregulation during periods of movement below and above the thermocline using a commonly employed empirical expression that describes the instantaneous rate of change in RM temperature ($dT_{RM}\,dt^{-1}$) relative to ambient temperature (T_a):

$$\frac{dT_{RM}}{dt} = k(T_a - T_{RM}), \qquad (1)$$

where t is time (min), and k (Δ°C min^{-1} °C^{-1}) is the thermal rate coefficient, a value encompassing all bodily or environmental conditions that affect heat transfer (Neill and Stevens, 1974; Neill *et al.*, 1976; Brill *et al.*, 1994; Dewar et al., 1994b; Bernal *et al.*, 2001b). Integrating equation (1) with respect to t yields:

$$\frac{[T_a - T_{RM}(t)]}{[T_a - T_{RM}(0)]} = e^{-kt}, \qquad (2)$$

where T_a is the water temperature at depth or at the surface, T_{RM} (t) is the RM temperature at time t and T_{RM} (0) is the T_{RM} prior to a change in T_a. Rearrangement of equation (2) enables k to be calculated for any time period,

$$k = -\frac{1}{t}\ln\frac{T_a - T_{RM}(t)}{T_a - T_{RM}(0)} \qquad (3)$$

and equation (3) can be transformed into a linear function with the slope –k:

$$\ln|T_a - T_{RM}(t)| = \ln|T_a - T_{RM}(0)| - k(t). \qquad (4)$$

Data (i.e. depth and temperature) were divided into two major categories: descents and ascents. The former included time periods over which depth increased and the time-at-depth, and the latter included time periods over which depth decreased and the time-at-surface (Figure 2a). For each descent in which T_a decreased below 16 °C (i.e. temperature associated with the thermocline; Figure 2a and Supplementary Figure S1), we calculated the k value ($k_{descent}$) for the time-period beginning with and including the initial decrease in T_a (i.e. non-steady state), and ending when either T_a and T_{RM} both reached a steady-state condition or when an ascent was initiated. Similarly, for each ascent in which T_a increased above 16 °C, we calculated the k value (k_{ascent}) for the time period beginning with and including the time period when the T_a began increasing after some time-at depth, and ending when the T_a and T_{RM} both reached steady-state or a new descent was initiated. Last, due to fine scale movements during long periods spent at depth or the surface, we calculated the T_a for the time-at-depth ($T_{a\text{-}descent}$) and the time-at-surface ($T_{a\text{-}ascent}$) as:

$$T_{a-descent} = \frac{\text{mean } (T_a) + \text{ minimum}(T_a)}{2}, \qquad (5)$$

$$T_{a-ascent} = \frac{\text{mean } (T_a) + \text{ maximum}(T_a)}{2}, \qquad (6)$$

where mean, minimum, and maximum pertain only to the T_a measurements during a specific descent or ascent interval.

To facilitate comparisons between swordfish and other species, all k values are reported in absolute terms (Carey and Teal, 1969; Neill and Stevens, 1974, Neill *et al.*, 1976; Dewar *et al.*, 1994; Bernal *et al.*, 2001b). We report the ratio of k_{ascent} to $k_{descent}$ to express the difference between rates of RM temperature change during exposure to disparate ambient conditions and as a metric of thermoregulatory capacity (Brill *et al.*, 1994). Unless otherwise noted, all values are mean ± standard error.

In order to further assess the capacity for physiological thermoregulation, we used a supplementary, predictive modelling approach, which was similar to that employed previously for bigeye tunas (*Thunnus obesus*) (Holland *et al.*, 1992; Holland and Sibert, 1994; Malte *et al.* 2009). We calculated k values from equation (1) as applied to non-instantaneous, consecutive vertical movement cycles, or steady and non-steady state conditions (i.e. entire tracking period). The equation (1) was amended to include the theoretical temperature change attributed to metabolic heat production (T_{met}) through time ($dT_{met}\,dt^{-1}$; °C):

$$\frac{dT_{RM}}{dt} = k(T_a - T_{RM}) + \frac{dT_{met}}{dt}. \qquad (7)$$

Four different models of heat transfer between T_{RM} and T_a were employed to determine the number of k values (from 1 to 3 k values) required to best predict the measured T_{RM} for the entire tracking period. The following possibilities for k were examined:

Model 1: k = constant; The k_1 heat transfer mode was permanently employed (Holland *et al.*, 1992; Holland and Sibert, 1994).

Model 2: k_1 if $T_a < T_{RM}$; k_2, if $T_a \geq T_{RM}$; Two heat transfer modes, k_1 and k_2, were differentially employed based on the absolute difference between T_a and T_{RM} (Holland and Sibert, 1994).

Model 3: k_1 if $T_a - T_{RM} < T_{crit}$; k_2 if $T_a - T_{RM} \geq T_{crit}$; Two heat transfer modes, k_1 and k_2, were differentially employed based on
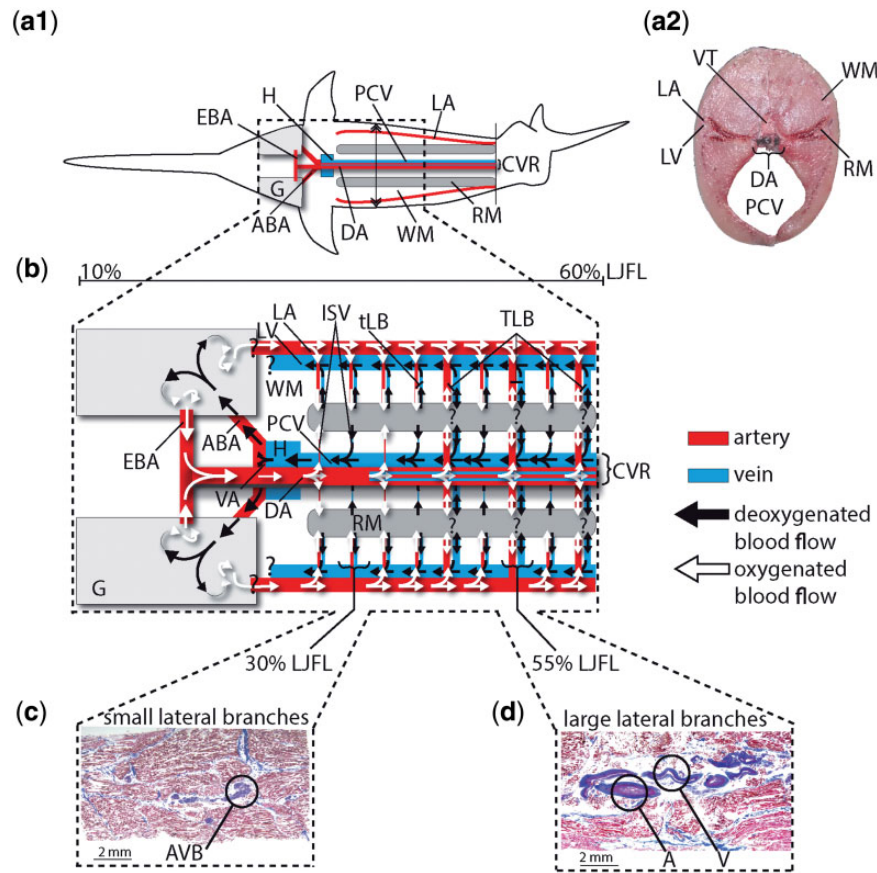
Figure 1. (a) Swordfish showing RM position and vasculature as described by Carey (1990) [Left panel a1: dorsal-view. Right Panel a2: transverse section taken at midbody region, as demarcated by double-headed arrow]. (b) Updated diagram of vascular anatomy with proposed direction of blood flow to and from the RM. The "?" shows unknown origin, drainage, or trajectory of blood vessels. Histological sections stained with trichrome of the (c) thin-walled and (d) thick-walled lateral branches from a 99 cm LJFL swordfish. Abbreviations: A, representative artery; ABA, afferent branchial arteries; AVB, arterio-venous bundles; CVR, central vascular rete; DA, dorsal aorta; EBA, efferent branchial arteries; G, gills; H, heart; ISV, intersegmental vessels; LA, lateral artery; TLB, thick-walled lateral branches; LV, lateral vein; PCV, post-cardinal vein; RM, red muscle; tLB, thin-walled lateral branches; WM, white muscle; V, representative vein; VA, ventral aorta; VT, vertebrae.

an optimized, critical temperature difference (T_{crit}) between T_{RM} and T_a (Holland *et al.*, 1992; Holland and Sibert, 1994).

Model 4: k_1 if $T_a - T_{RM} < T_{crit}$; k_2 or k_3 if $T_a - T_{RM} \geq T_{crit}$. We employed k_2 if T_a at time t was below the mean surface ($\bar{T}_a$) (i.e. average of T_a measurements recorded at depths shallower than the thermocline at ~70 m; Sepulveda *et al.*, 2010; Figure 2a and Supplementary Figure S1), and a depth deeper than 70 m. We employed k_3 if $T_a(t)$ was above the mean surface $\bar{T}_a$ and depth was shallower than 70 m. In other words, we differentially employed the three heat transfer modes (k_1, k_2, and k_3) based on an optimized T_{crit} between T_{RM} and T_a, as well as the depth (m) of the individual relative to the thermocline. More specifically, k_1 was used when the thermal gradient ($T_a - T_{RM}$) was less than the optimized T_{crit}; but if the thermal gradient was greater than the optimized T_{crit}, then either k_2 or k_3 were used. The k_2 mode was used if the individual was near or below the thermocline, as indicated by T_a values that were cooler than the average surface $\bar{T}_a$ throughout the tracking period and a recorded depth below 70 m. The k_3 mode was used if the individual was in the warm waters above the thermocline (i.e. T_a values $\geq$ the average $\bar{T}_a$ recorded during the time at the surface and depth was shallower than 70 m). The k_3 option was added to Model 4 to account for

activity-dependent changes in the rate of heat transfer during long-duration surface intervals (time-at-surface). Swordfish may exhibit different activity levels while at the surface (e.g. periods of high speed swimming while feeding, steady swimming during the night, and slow swimming while basking at the surface during the day), which will affect T_{met} or blood flow to the RM, and consequently k and $dT_{RM}\ dt^{-1}$ (equation 7) (Brill *et al.*, 1994).

We estimated all parameters (i.e. k, T_{met}, T_{crit}) through heuristic methods of local optimization (i.e. hill-climbing), using numerical ranges obtained from published values for other active fishes (i.e. k: from 0 to 1 $\Delta°C\ min^{-1}\ °C^{-1}$; T_{met}: from 0 to 5 °C; T_{crit}: from −20 to 20 °C; Carey and Teal, 1969; Carey and Lawson, 1973; Graham, 1974; Neill *et al.*, 1976; Carey *et al.*, 1985; Carey, 1990; Dewar et al., 1994b; Holland and Sibert, 1994; Bernal *et al.*, 2001; Kitagawa and Kimura, 2004; Malte *et al.*, 2009). The T_{met} was assumed to be constant throughout the vertical movement cycle, as there were no significant differences in the rate of vertical change (i.e. the minimum vertical swimming speed in cm/s) between descents and ascents (t-test, $p = 0.13$). The differential equation (7) was solved in Matlab at each 1-minute time step and optimized parameters were selected based on the least squared
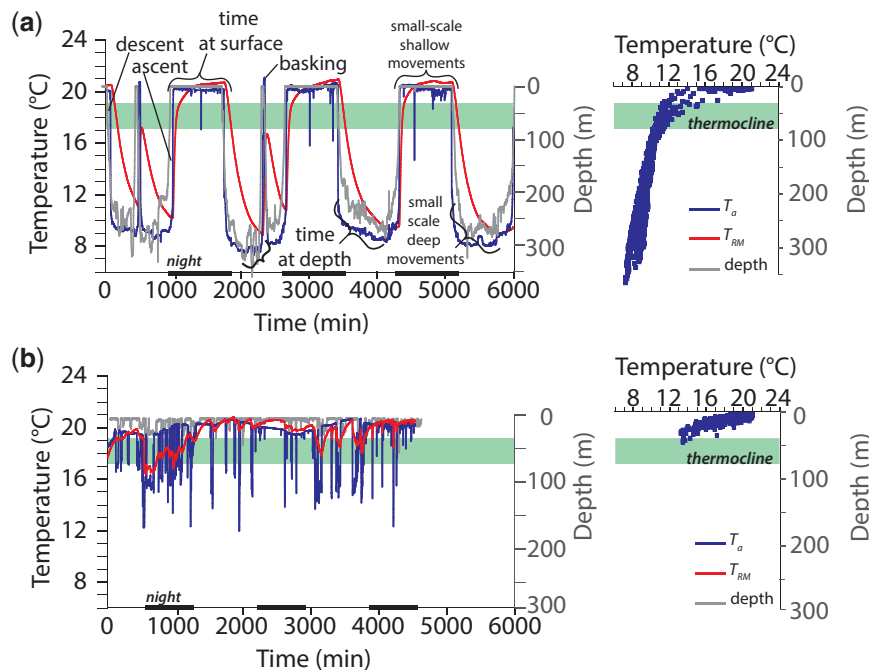
Figure 2. Representative vertical movement patterns of free-swimming swordfish (left panel) and water temperature-depth profiles (right panel) obtained from archival tags for (a) swordfish (91 kg, ID no. 1) displaying extensive vertical movements and (b) a surface-orientated swordfish (109 kg, ID no. 5). T_{RM}, red muscle temperature; T_a, ambient temperature.

difference between the observed (T_{RMo}) and predicted (T_{RMp}) RM temperature measurement (i), or the residual sum of squares (RSS; Malte *et al.*, 2009):

$$\text{RSS} = \sum_{i=1}^{n} \left(T_{RMo}(i) - T_{RMp}(i) \right)^2. \tag{8}$$

The best model was selected as that producing the lowest RSS with the fewest number of parameters. For example, if in Model 3, T_{crit} proved unnecessary, local optimization would set T_{crit} equal to 0 and the RSS for Model 2 and Model 3 would be equal (i.e. Model 2 = Model 3); in this instance Model 2 would be chosen over Model 3. Similarly, if in Model 4 k_3 proved to be unnecessary, local optimization would cause the k_3 value to equal either k_1 or k_2 (i.e. 2 k values, Model 3 = Model 4), and Model 3 would be selected as the best-fit model.

For all analyses, we used data from only the five swordfish showing diel, vertical movements in our heat-transfer analyses.

Results

RM-associated vasculature anatomy

The ventral aorta (VA), or the principal vessel exiting the heart, branched into smaller afferent branchial arteries (ABA) that entered the gill arches. The EBAs exited the gills to join the DA, which was at this point paired. The DA merged posteriorly to form a single centrally positioned (i.e. under the vertebrae) vessel. The DA branched between 40 and 70% LJFL to send lateral intersegmental arteries towards the RM at every ∼1–2 vertebral segments (Figure 1b). Similarly, the small, lateral intersegmental veins, which drained from the RM, were traced towards the vertebrae where they joined the PCV (Figure 1b). The PCV travelled anteriorly from the caudal vein and enlarged to form the common cardinal sinus that joined the sinus venosus at the

pericardial cavity. A putative central rete, previously described by Carey (1990) as "one to six layers of vessels", was evident posterior to the celiacomesenteric artery and consisted of the DA, PCV, and four or more smaller adjacent arteries and veins, all of which travelled in contact with each other, directly beneath the vertebrae and along the length of the fish (Figure 1b).

In addition to the central blood supply (i.e. via the DA and PCV), swordfish possess an additional, lateral, or subcutaneous, route of systemic blood supply to and from the RM. A large LA seemingly originated from a plexus of EBAs and exited the opercular cavity beneath the scapular process of the pectoral girdle (Figure 1b). The LAs (i.e. one on each side of the body) travelled posteriorly along the body, within the WM (1 × 2 cm beneath the skin) and near the horizontal septum. A lateral vein (LV) ran in tandem with the LA towards the caudal peduncle (Figure 1b). We could not determine the exact origin or termination of the LV, but our observations suggest that it could descend medially towards the heart at the scapular process. The LA and LV were surrounded by a shared sheath of collagenous connective tissue.

As the LA and LV ran anterio-posteriorly along the body from 30 to 85% LJFL, they divided, sending small, thin-walled vessel branches through the horizontal septum into the RM (Figure 1b). Histological sections from these branches, revealed that each contained small collections of juxtaposed arterioles and venules (i.e. arterio-venous bundle; area ∼1 mm^2; Figure 1b and c). The number and frequency of these branch-points from the LA and LV appeared to vary between smaller (≤90 cm LJFL) and larger individuals (>120 cm LJFL), but generally occurred every 1–2 cm. There were also more sizeable, thicker-walled lateral vessel branches (e.g. 50, 55, and 60% LJFL) in larger individuals, each of which was composed of several arteries and veins separated by connective tissue and fat cells (Figure 1b and d).

Ambient and body temperature

We obtained time-series of T_a and T_{RM} data from six free-swimming swordfish in the Southern California Bight ($\sim$90–140 kg). Five of the six individuals (ID nos. 1,2,3,4, and 6) displayed diel, vertical movement behaviour. They rapidly descended (37 $\pm$ 9 min) from the surface to $\sim$375 m at dawn, spent the duration of the day at depth (time-at-depth: 680 $\pm$ 55 min), and rapidly ascended (22 $\pm$ 5 min) to the surface at dusk, where they spent the duration of the night (time-at-surface: 773 $\pm$ 24 min) (Figure 2a and Supplementary Figure S1). Some individuals also showed short-lived (27 $\pm$ 4 min) surface basking events during the day (Figure 2a and Supplementary Figure S1). On average, the five swordfish spent 69 $\pm$ 16% of the night at or above the thermocline (above 70 m; mean T_a 19.6 $\pm$ 0.8 °C) and 66 $\pm$ 16% of the day below the thermocline (mean T_a of 8.8 $\pm$ 0.1 °C) (Supplementary Figure S1). This contrasts with the surface-oriented behaviour exhibited by swordfish # 5 ($\sim$110 kg), which mostly remained above 25 m and spent $\sim$98% of the tracking period at a $T_a \geq 16$ °C (Figure 2b and Supplementary Figure S1f).

RM endothermy

The T_{RM} during descents and time-at-depth was generally elevated above T_a during prolonged periods at depth (e.g. $\sim$8–13 h). During this time, however, the T_{RM} slowly decreased until it approached and approximated the T_a at depth (Figures 2a and 3a, and Supplementary Figure S1). The T_a surpassed T_{RM} only during rapid ascents, but this reversal in thermal gradient was transient (e.g. average of 42 $\pm$ 17 min out of 773 $\pm$ 24 min at surface, or 20% of the total tracking period for $n = 5$ swordfish), and the T_{RM} came to closely approximate the T_a at the surface. During steady-state conditions (i.e. ΔT_a and $\Delta T_{RM} < 0.1$ °C for $\geq$ 10 min; Neill et al., 1976) the T_{RM} did not differ from the T_a at depth (t-test, $p = 0.15$) or at the surface (t-test, $p = 0.32$), nor did the average T_x differ when at depth ($T_x = 0.58 \pm 0.57$ °C, $n = 5$) or at the surface ($T_x = 0.71 \pm 0.87$ °C, $n = 5$) (t-test, $p = 0.8$).

To better visualize the temporal distribution of T_a vs. T_{RM} during both steady-state and non-steady state periods (i.e. during vertical movement), T_a and T_{RM} measurements were binned into four categories: (i) values recorded at depth ($\leq$8–12 °C); (ii) values recorded at the lower boundary of the thermocline (12–16 °C); (iii) values recorded at the upper boundary of the thermocline (16–20 °C); and (iv) values recorded at the surface (20–24 °C) (Supplementary Figure S1). This analysis showed that T_a and T_{RM} values were in the warmest category (i.e. at surface, 20–24 °C) for a similar percentage of the tracking period (both $\sim$59%), suggesting T_{RM} was closely tracking T_a when swordfish were above the thermocline. There was, however, a greater disparity in the distribution and number of T_{RM} ($\sim$4% of the total tracking period) and T_a ($\sim$20% of the total tracking period) measurements in the coldest category (i.e. $T_a \leq 8$–12 °C), suggesting that T_{RM} does not closely track T_a when swordfish were below the thermocline.

Physiological thermoregulation

Our instantaneous heat transfer analysis (equation 4) using non-steady state intervals showed that swordfish RM warmed 13 $\pm$ 4 times faster during ascents than it cooled during descents (mean $k_{ascent} = 0.0572 \pm 0.0130 \, \Delta$°C min^{-1} °C^{-1} vs.ersus mean $k_{descent} = 0.0053 \pm 0.0008 \, \Delta$°C min^{-1} °C^{-1}; Mann Whitney Rank Sum Test k_{ascent} vs. $k_{descent}$, $p < 0.01$; Table 1 and Figure 3a and b).

Our non-instantaneous heat transfer analysis (Equation 7), including steady and non-steady state intervals, also showed that more than one k value was necessary to best describe heat transfer during vertical movements (Table 1; Figure 3c–f). Model 1, which used a single, permanently employed k_1 value, underestimated the T_{RM} during ascents and overestimated the T_{RM} during steady-state conditions at the surface. Models 2 and 3, which variably switched between k_1 and k_2 values, tended to overestimate the T_{RM} during descents and the steady-state conditions at depth. Model 4, which switched between k_1, k_2, and k_3 values, was the most accurate predictor of T_{RM} in swordfish.

For the five swordfish showing diel, vertical movements, the average rates of heat transfer for Model 4 were $k_1 = 0.0049 \pm 0.0006 \, \Delta$°C min^{-1} °C^{-1}, $k_2 = 0.0292 \pm 0.0046 \, \Delta$°C min^{-1} °C^{-1}, and $k_3 = 0.0447 \pm 0.0048 \, \Delta$°C min^{-1} °C^{-1}. Values for k_1 were similar to $k_{descent}$, and values for k_2 and k_3 were similar to k_{ascent} (paired t-test, all $p > 0.05$; Table 1). The optimized k_1 values were significantly smaller than k_2 and k_3 and while k_2 and k_3 were not significantly different between swordfish, these values were always unequal within individuals (k_1 vs. k_2 paired t-test, $p = 0.01$; k_1 vs. k_3 paired t-test, $p < 0.01$; k_2 vs. k_3 paired t-test, $p = 0.13$; Table 1; Figure 3f). A single k_1 value was employed for 92 $\pm$ 6% of the tracking period during descents, time-at-depth, and steady-state periods during the time-at-surface (Figure 3f). The k_2 and k_3 values were employed only during 2 $\pm$ 2% and 6 $\pm$ 5% of the tracking period, respectively. As a consequence of Model 4 rules, k_2 was used during initial ascents, and k_3 was used near the end of ascents and during any shallow (i.e. < 70 m), short duration descents occurring throughout the time-at-surface (Figure 3f). We calculated the ratio of heating to cooling for the Model 4 results by averaging the statistically similar k_2 and k_3 values, and dividing that mean by k_1 [mean (k_2, k_3) . k_1^{-1}], which indicated that the RM warmed 8 $\pm$ 1 times more rapidly than it cooled.

Additionally, we applied our heat transfer models to the data collected on free-swimming swordfish by Carey (1990): a $\sim$32 kg (ID no. 10) swordfish captured in the warm waters of the Florida Straits and a $\sim$140 kg swordfish (ID no. 11) captured in the cooler, more northern waters off of Georges Bank (Carey, 1990). Both fish exhibited diel, vertical movement behaviour, spending the evening hours in the upper-mixed layer and the majority of daylight hours beneath the thermocline (>200 m; Carey, 1990; Figure 4). The model that most accurately predicted RM temperature (i.e. Model no. 4) showed that both fish used a low-heat transfer mode (Swordfish no. 10, $k_1 = 0.0068$; Swordfish no. 11, $k_1 = 0.0037$; Table 1; Figure 4) during descents and then switched to a high-heat transfer mode during ascents (Swordfish no. 10, $k_2 = 0.0107$; $k_3 = 0.0123$; Swordfish no. 11, $k_2 = 0.0261$; $k_3 = 0.0690$; Table 1; Figure 4). In agreement with the observations made by Carey (1990), the results of Model 4 indicate that the $\sim$32 kg swordfish warmed nearly twice as fast as it cooled [mean (k_2, k_3) . $k_1^{-1} = 1.69$], whereas the $\sim$140 kg swordfish warmed 10 times more quickly than it cooled [mean(k_2, k_3) . $k_1^{-1} = 12.85$] (Table 1).

In summary, it would appear that despite marked differences in body size ($\sim$32 vs. > 100 kg), as well as differences in thermal stratification between the waters of the northwest Atlantic Ocean, southwest Atlantic Ocean, and Eastern Pacific Ocean, thermodynamic Model 4 is able to estimate a capacity for physiological thermoregulation in free-swimming swordfish.
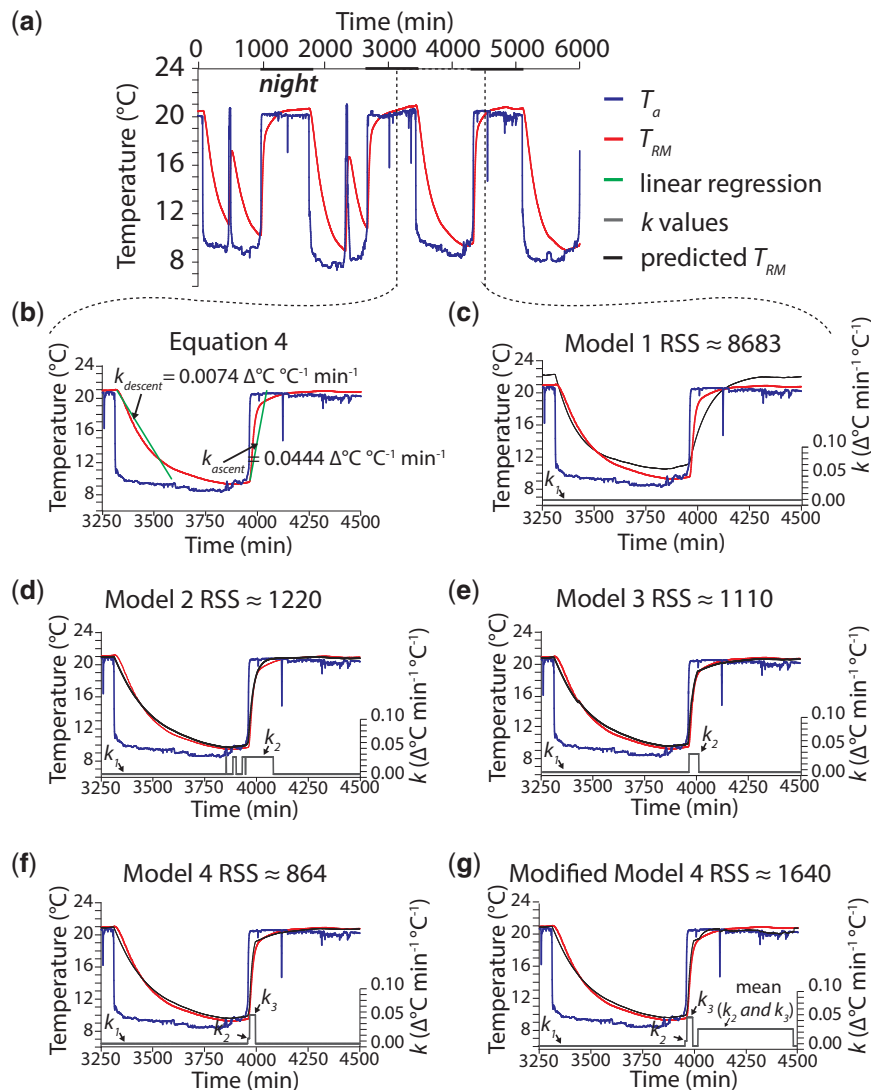
Figure 3. Representative vertical movement patterns for a 91-kg swordfish (ID no. 1). (a) Entire tracking period showing T_{RM} and T_a during long-duration descents, surface intervals, and basking events. The area inside the dashed lines represent the region presented in panels b-g. (b) Results for equation (4). Straight diagonal lines are the linear regression lines used to calculate the $k_{descent}$ and k_{ascent} values for each respective interval. Results for equation (7) are shown for (c) Model 1, (d) Model 2, (e) Model 3, (f) Model 4, and (g) a modified Model 4 using a high-heat transfer mode (mean of k_2 and k_3 values) at the surface. In c-g, the secondary axis corresponds to labeled k values. The RSS for the entire track is provided for each model (Table 1). T_{RM}, red muscle temperature; T_a, ambient temperature; k, thermal rate coefficient.

Discussion

Our data corroborate and expand previous observations of two distinct blood flow pathways to the RM (Carey, 1990) and provide a more detailed description of the central vascular rete and lateral circulation. Despite the presence of two circulatory routes to the RM, as well as the presence of anatomical structures resembling heat-exchanging retia, our *in vivo* temperature data and that of others (Carey and Gibson, 1987; Carey, 1990) suggest that swordfish have a reduced capacity for RM endothermy when compared with tunas, lamnid sharks, and the common thresher shark, all of which possess more complex or larger retia (Carey and Teal, 1966; Carey *et al.*, 1971; Bone and Chubb, 1983; Graham *et al.*, 1983; Dickson, 1994; Dewar *et al.*, 1994; Patterson *et al.*, 2011). Our thermodynamic models, which predict how

changes in T_a alter T_{RM} in free-swimming swordfish, are able to confirm, however, that during descents and ascents swordfish alter rates of whole-body heat transfer (Table 1; Figure 3b and f) and thus have the ability to physiologically thermoregulate, as suggested by Carey (1990).

RM endothermy: steady-state RM temperatures and anatomy

The diel vertical movement patterns shown in Figure 2a and Supplementary Figure S1 have been recognized as a foraging tactic that allows swordfish to exploit the vertically migrating species that compose the DSL both during the day (when the DSL descends to deep, cold waters; 250–350 m, ≤8 °C) and at night

Table 1. Heat transfer in the deep body (i.e. red muscle) of free-swimming swordfish.

Mass—kg (Fish no.)[e]	T_a Range (°C)	$k_{descent}$[a] Δ°C min^{-1} °C^{-1} [n][b]	k_{ascent}[a] min^{-1} °C^{-1} [n][b]	Model	k_1[a] Δ°C min^{-1} °C^{-1}	% time k_1 used[c]	k_2[a] Δ°C min^{-1} °C^{-1}	% time k_1 used[c]	k_3[a] Δ°C min^{-1} °C^{-1}	% time k_1 used[c]	T_m (Δ°C min^{-1})	T_{crit} (Δ°C)	RSS[d]
109 kg[e] (5)	12–21	0.0465 ± 0.0216 [6]	0.0364 ± 0.0118 [10]	1	0.0116	100					0.0058		293
				2	0.0122	60	0.0099	40			0.0068		283
				3	0.0112	99	0.0007	1			0.0061	2.39	265
				4	0.0125	99	0.0059	1	0.1497	0.1	0.0061	1.99	243
91 kg (1)	7–21	0.0074 ± 0.0004 [6]	0.0443 ± 0.0024 [5]	1	0.0088	100					0.0164		8683
				2	0.0053	89	0.0350	12			0.0024	1.39	1220
				3	0.0055	96	0.0372	4			0.0032		1110
				4	0.0056	96	0.0143	2	0.0549	2	0.0034	1.44	862
109 kg (2)	7–23	0.0065 ± 0.0011 [6]	0.0577 ± 0.0089 [6]	1	0.0076	100					0.0231		11008
				2	0.0048	83	0.0341	17			0.0059		1244
				3	0.0048	80	0.0339	21			0.0060	−0.14	1240
				4	0.0048	82	0.0271	5	0.0368	13	0.0061	−0.07	1199
109 kg (6)	8–19	0.0054 ± 0.0005 [7]	0.0263 ± 0.0071 [6]	1	0.0114	100					0.0256		1804
				2	0.0053	71	0.0407	29			0.0000		332
				3	0.0063	93	0.0432	7			0.0059	1.43	210
				4	0.0069	94	0.0235	2	0.0512	4	0.0084	1.73	195
127 kg (3)	7–22	0.0040 ± 0.0006 [5]	0.1042 ± 0.0227 [5]	1	0.0069	100					0.0150		12533
				2	0.0037	73	0.0369	27			0.0000		2505
				3	0.0041	97	0.0491	3			0.0027	2.13	1884
				4	0.0042	97	0.0436	1	0.0503	3	0.0028	2.12	1876
136 kg (4)	7–23	0.0031 ± 0.0001 [4]	0.0532 ± 0.0111 [4]	1	0.0047	100					0.0165		12426
				2	0.0031	85	0.3160	16			0.0033		595
				3	0.0031	91	0.0325	9			0.0036	0.47	584
				4	0.0031	90	0.0375	2	0.0302	9	0.0035	0.32	580
32 kg (10) (Carey, 1990)	7–25	0.0057 ± 0.0008 [3]	0.0248 ± 0.0009 [3]	1	0.0087	100					0.0144		116
				2	0.0066	68	0.0125	32			0.0047		41
				3	0.0069	26	0.0112	74			0.0097	−4.16	35
				4	0.0068	25	0.0107	45	0.0123	30	0.0096	−4.31	32
140 kg (11) (Carey, 1990)	6–19	0.0026 ± 0.0000 [2]	0.0327 [1]	1	0.0057	100					0.0130		148
				2	0.0033	72	0.0195	28			0.0021		33
				3	0.0034	70	0.0193	30			0.0025	−0.22	33
				4	0.0037	93	0.0261	5	0.0690	2	0.0038	1.08	22

T_{RM}, RM temperature; T_a, ambient temperature; T_m, temperature produced per minute due to metabolic heat production; T_{crit}, critical temperature difference that specifies switching between possible k values (k_1, k_2 or k_3).

[a]Mean + SEM calculated by linear regression (equation 4) for each dive and surface interval per fish.

[b]Total number of descents or surface intervals analysed.

[c]Percent of time during the dive track where k value was employed relative to the entire time of the dive track for each model.

[d]Residual sum of squares (lower values indicate better fit of Model).

[e]Indicates surface-orientation (i.e. does not display diel movement patterns).

(when the DSL ascends to the warmer, surface layer; $\geq 18\,°C$) (Carey and Robinson, 1981; Carey and Gibson, 1987; Carey, 1990; Takahashi *et al.*, 2003; Sepulveda *et al.*, 2010; Dewar *et al.*, 2011). Previous recordings of *in vivo* muscle temperature using acoustic telemetry (Carey and Gibson, 1987; Carey, 1990) and our findings, using archival tags, reveal that swordfish are unable to maintain a T_{RM} consistently above T_a during prolonged time periods at depth ($\sim 8\,°C$) or at the surface ($\sim 20\,°C$). Instead, during movements through the thermocline, the T_{RM} of swordfish fluctuates by more than $\sim 12\,°C$ until reaching an equilibrium temperature that is similar to ambient conditions at depth or at the surface ($T_{RM} - T_a = T_x < 1\,°C$; Figures 2a and 3, and Supplementary Figure S1).

Thus, while swordfish have evolved the hallmarks of RM endothermy (e.g. medial RM position and associated vascular rete; Carey, 1990; Block and Finnerty, 1994; Dickson, 1994; Bernal *et al.*, 2009); they do not appear to maintain a steady-state T_x typical of tunas, lamnid sharks, or the common thresher shark (e.g. $T_x \geq 2.7\,°C$; Dickson, 1994). Even though our anatomical findings in swordfish, like those of Carey (1990) show that at least some of the systemic blood flow to the RM is through a centralized vascular rete composed of up to six arteries and veins including the DA and PCV (Figure 1a and b), our observations also verify that their central rete is markedly smaller in size and complexity than that of most tunas (Graham, 1974; Stevens *et al.*, 1974). Although the central rete of swordfish may act as a rudimentary heat exchanger, its relative simplicity may explain why the core body temperatures of free-swimming swordfish are lower than those reported for fishes with RM endothermy (Carey and Teal, 1966, 1969; Carey *et al.*, 1971; Carey and Gibson, 1987; Carey, 1990; Block and Finnerty, 1994; Dickson, 1994; Graham and Dickson, 2004; Bernal *et al.*, 2009).

Physiological thermoregulation: non-steady-state RM temperature and anatomy

The ability of swordfish to forage on those organisms comprising the DSL both above and below the thermocline is likely facilitated by the ability to control rates of whole-body heat transfer (i.e. the capacity for physiological thermoregulation first described in tunas by Dizon and Brill, 1979a,b). Despite the low capacity for RM endothermy in swordfish, our models show that multiple thermoregulatory modes (i.e. *k* values) are necessary to simulate T_{RM} during vertical movements (Table 1; Figure 3 and Supplementary Figure S1). Swordfish display a low-heat transfer mode ($k_{descent}$, k_1) during descents from the surface and throughout the time-at-depth (Figure 3a, b, and f). This results in slow rates of T_{RM} decrease, which permits the T_{RM} to remain elevated above ambient for upwards of 8 h (i.e. non-steady state conditions; Figure 3a, b, and f). During ascents back to the warm upper mixed layer (Figure 3a, b, and f), swordfish switch to a high-heat transfer mode (k_{ascent}, k_2, k_3), which rapidly increases T_{RM} due to the transfer of heat from the water to the fish. During prolonged periods at the surface, however, swordfish revert back to a low-heat transfer mode that may (when compared with a high-heat transfer mode) stabilize T_{RM} during the shallow, short-duration vertical movements, which are common during surface-foraging (Figure 3f vs. 3g) (Carey, 1990; Sepulveda *et al.*, 2010). Overall, our data suggest that during descents through the thermocline and while at depth, swordfish are able to alter their rates of whole-body heat transfer to effectively slow the decrease in T_{RM}

by ~ 8 [mean (k_2, k_3) . k_1^{-1}; Model 4] to 13 (k_{ascent} $k_{descent}^{-1}$) times during descents, as compared with the rate of increase in T_{RM} during ascents above the thermocline.

This capacity for physiological thermoregulation may play an important role in swordfish thermal ecology, as it likely permits the RM to operate at temperatures, which are warmer and more amenable to contractile performance, for a greater percentage of time within the vertical movement cycle (Supplementary Figure S1). During the initial descent and time-at-depth, the slow rate of RM cooling may allow swordfish to maintain faster sustained swimming speeds relative to other ectothermic species (e.g. bigeye thresher sharks, *Alopias superciliosus;* blue sharks, *Prionace glauca*) that also forage below the thermocline (Carey and Gibson, 1987; Nakano *et al.*, 2003; Donley *et al.*, 2007; Bernal *et al.*, 2009). Additionally, the RM may conductively warm some of the surrounding WM and temporarily enhance WM contractile performance during bouts of burst swimming (Johnston and Brill, 1984; Korsmeyer and Dewar, 2001; Bernal *et al.*, 2003). In contrast, the ability to rapidly re-warm the RM most likely reduces the time-at-surface during basking intervals ($\sim 20\,min$, Sepulveda *et al.*, 2010; Figure 2a), allowing swordfish to quickly return to depth and exploit the organisms of the DSL during the day (Carey and Robinson, 1981; Carey and Gibson, 1987; Carey, 1990; Takahashi *et al.*, 2003; Sepulveda *et al.*, 2010; Dewar *et al.*, 2011). The rapid RM re-warming may also allow swordfish to minimize any competitive disadvantage relative to surface-orientated fishes that have not experienced RM cooling (Altringham and Block, 1997; Donley *et al.*, 2007); making it important for prey search and capture, as well as predator avoidance (Stillwell and Kohler, 1982). Last, the ability to control heat transfer rates during ascents and surface intervals may serve to prevent the possibility of deleterious overheating (Neill *et al.*, 1976; Dizon and Brill, 1979a,b; Brill *et al.*, 1994; Dewar *et al.*, 1994b; Altringham and Block, 1997). For example, if swordfish employed a single, low-heat transfer mode (i.e. see Model 1; i.e. k_1; Figure 3c) during the entire vertical movement cycle, our models predict a marked increase in the time to re-warm the RM, as well as continued warming to temperatures far above the T_{RM} observed in free-swimming individuals.

The capacity for physiological thermoregulation in swordfish is likely associated with the presence of two putative circulatory routes (i.e. central and lateral circulation), which operate at different heat-exchange efficacies, to perfuse the RM. Although we observed the formation of small arterio-venous bundles extending from the large LA and newly described LV into the RM, the small surface area of blood-vessel contact within bundles makes effective venous to arterial heat exchange unlikely (Carey and Teal, 1966; Dickson, 1994; Figure 1b). More specifically, swordfish may slow RM cooling by routing blood flow through the central vascular rete to effectively retain RM-produced heat (Carey, 1990; Table 1; Figure 3b and f). Swordfish may then expedite RM re-heating when T_{RM} is below T_a by routing blood flow around the rete and through the lateral circulation to quickly harness heat from the environment (Carey, 1990; Table 1; Figure 3b and f).

All swordfish (displaying vertical movement behaviour) in our study, and the ~ 32 and $140\,kg$ individuals observed by Carey (1990) (Figure 4), displayed physiological thermoregulation during diel, vertical movements, but there were some differences in the calculated heating to cooling ratios, possibly related to body size (Table 1; Figure 4 and Supplementary Figure S1). For
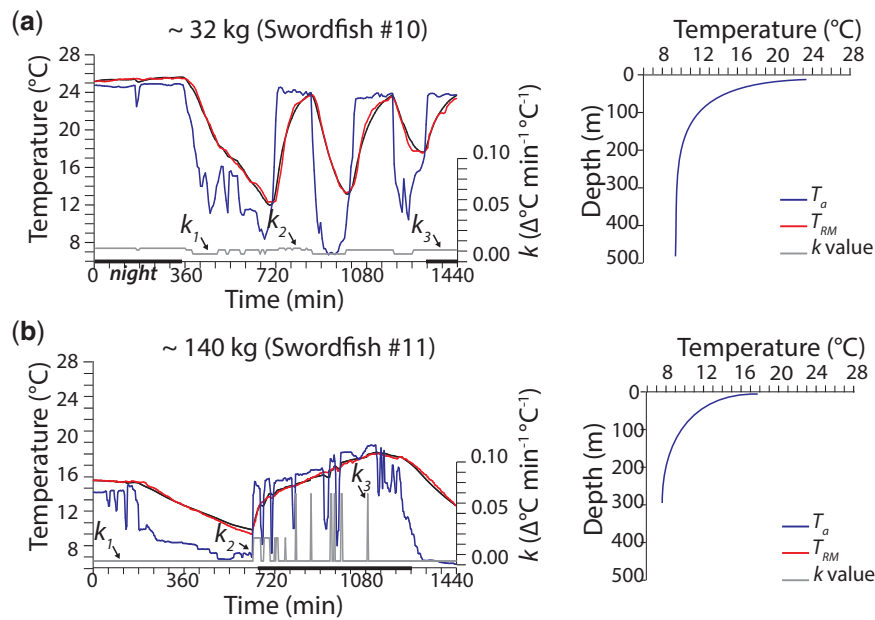
Figure 4. Vertical movement patterns for swordfish obtained by Carey (1990): (a) ~32 kg swordfish (no. 10) in the Florida Straight and (b) ~140 kg swordfish off Georges Bank (no. 11). Left panel shows the use of Model 4 (this study) to predict deep-body temperature. Right panel shows the estimated temperature-depth profile of the water column. T_{RM}, red muscle temperature; T_a, ambient temperature; k, thermal rate coefficient.

example, the different ratios observed between Carey's (1990) small Floridian fish [mean $(k_2, k_3) \cdot k_1^{-1}=2$], and the larger, Georges Bank fish [mean $(k_2, k_3) \cdot k_1^{-1}=10$], likely reflect the need of the former to utilize a low-heat transfer thermoregulatory mode more often because of lower thermal inertia, which is generated by greater conductive heat transfer due to smaller girth and greater convective heat transfer due to smaller vascular heat-exchanging retia (Dickson, 1994).

Additional variability is likely a consequence of differences in the position of the thermistor or swimming behaviour. It is important to consider that all the temperature measurements for free-swimming swordfish have been obtained by the insertions of external thermistors via a harpoon (Carey and Gibson, 1987; Carey 1990; our study); and because individuals were not recaptured, it is not possible to ascertain precise thermistor position relative to the RM. We contend, however, that changes in the route of blood flow to and from the RM are a major determinate of swordfish heat balance because: (i) there was no difference in minimum vertical speeds during descents and ascents, suggesting little variability in RM-powered sustained swimming; (ii) the heating to cooling ratios exceeded values that would be expected due to swimming-dependent changes in blood flow velocity alone (approximately five times; Stevens and Randall, 1967; Jones and Randall, 1978; Carey, 1990); and (3) there were no unexpected, short-lived spikes in deep-body temperature, as might be expected from any burst swimming (i.e. WM activity).

Swordfish thermal ecology

Swordfish experience daily, prolonged exposure to cold water (<8 °C) and also undertake extensive annual migrations to high latitudes (Carey, 1990; Watanabe *et al.*, 2015). The high degree of thermal tolerance exhibited by swordfish suggests that, for active, pelagic fishes, thermal niche expansion is not solely reliant upon

the degree to which a species is capable of maintaining a steady-state T_x across a range of ambient temperatures (i.e. RM endo-thermy), but rather, as proposed by Brill and Lutcavage (2001), the ability to regulate the rate of change in T_{RM} during migrations through different thermal environments, such as during rapid, vertical movements through the thermocline.

Among, active, large pelagic fishes, the capacity for physiological thermoregulation may significantly affect the ability to forage at depth. Swordfish are among the few active, large, pelagic teleost fishes that regularly undergo large diel, vertical movements to forage on the vertically migrating species within the DSL (Carey and Robinson, 1981; Carey and Gibson, 1987; Carey, 1990; Takahashi *et al.*, 2003; Musyl *et al.*, 2004; Bernal *et al.*, 2009; Sepulveda *et al.*, 2010; Dewar *et al.*, 2011; Figures 2a and 4, and Supplementary Figure S1). Although other species showing extensive daily vertical movements (e.g. bigeye tuna) make numerous (i.e. up to 20), short duration descents (<1 h) during the day (Holland and Sibert, 1994; Musyl *et al.*, 2003; 2004; Bernal *et al.*, 2009; Schaefer *et al.*, 2009), swordfish are distinct in that they make fewer descents (1–2) and spend much longer times-at depth (i.e. 6–10 h) (Carey and Robinson, 1981; Carey and Gibson, 1987; Carey, 1990; Takahashi *et al.*, 2003; Musyl *et al.*, 2004; Sepulveda *et al*, 2010; Dewar *et al.*, 2011). For bigeye tuna, the time-at-depth is thought to be limited by the change in T_{RM}, as they appear to maintain a T_{RM} that is greater than T_a and is at least 17 °C (Holland and Sibert, 1994; Malte *et al.*, 2009), the maintenance of which may safeguard oxygen transport to the RM, as well as muscle function (Brill, 1994; Holland and Sibert, 1994; Lowe *et al.*, 2001; Bernal *et al.*, 2009; Malte *et al.*, 2009). Swordfish, like bigeye tunas, must also cope with cold waters and low dissolved oxygen concentrations during movement below the thermocline (Carey and Robinson, 1981; Carey and Gibson, 1987; Carey, 1990; Brill and Lutcavage, 2001; Takahashi *et al.*, 2003; Musyl *et al.*, 2004; Bernal *et al.*, 2009; Sepulveda *et al.*, 2010; Dewar *et al.*, 2011).

Due to the large magnitude of observed fluctuations in the T_a and T_{RM} ($\Delta T_a \geq 16\,°C$, $\Delta T_{RM} \approx 12\,°C$) of free-swimming swordfish, it will be interesting to determine how temperature may influence oxygen delivery to the RM, or its contractile mechanics.

To date, the effects of extreme temperature fluctuations on sustained swimming capacity in swordfish remain unknown. Work on several pelagic fishes, that possess the capacity for RM endothermy, reveals substantial declines in RM performance and presumably sustained swimming capacity, with decreasing temperatures (Altringham and Block, 1997; Bernal *et al.*, 2005; Donley *et al.*, 2007, 2012). For those species with RM endothermy, contractile performance appears to be constrained within a narrow range of RM temperatures (i.e. $< \Delta 10\,°C$; Altringham and Block, 1997; Bernal *et al.*, 2005; Donley *et al.*, 2007; Syme and Shadwick, 2011; Donley *et al.*, 2012). Despite presence of retia and the capacity for physiological thermoregulation in swordfish, the T_{RM} fluctuates drastically (~ 8–$20\,°C$), suggesting the RM must operate over a broader thermal range.

Future work should, therefore, focus on quantifying the rates of oxygen uptake and offloading and performance of swordfish RM under varying thermal regimes to better determine if the capacity for physiological thermoregulation enhances sustained swimming capacity and possibly foraging success beneath the thermocline.

Supplementary data

Supplementary material is available at the *ICESJMS* online version of the article.

References

Abascal, F. J., Mejuto, J., Quintans, M., and Ramos-Cartelle, A. 2010. Horizontal and vertical migrations of swordfish in the Southeast Pacific. ICES Journal of Marine Science, 67: 466–474.

Altringham, J. D., and Block, B. A. 1997. Why do tunas maintain elevated slow muscle temperatures? Power output of muscle isolated from endothermic and ectothermic fish. Journal of Experimental Biology, 200: 2617–2627.

Bennett, A. F. 1984. Thermal dependence of muscle function. American Journal of Physiology, 247: R217–R229.

Bernal, D., Dickson, K. A., Shadwick, R. E., and Graham, J. B. 2001. Review: Analysis of the evolutionary convergence for high performance swimming in lamnid sharks and tunas. Comparative Biochemistry and Physiology, Part A, 129: 695–726.

Bernal, D., Sepulveda, C. A., and Graham, J. B. 2001b. Water-tunnel studies of heat balance in swimming mako sharks. Journal of Experimental Biology, 204: 4043–4054.

Bernal, D., Smith, D., Lopez, G., Weitz, D., Grimminger, T., Dickson, K., and Graham, J. B. 2003. Comparative studies of high performance swimming in sharks II. Metabolic biochemistry of locomotor and myocardial muscle in endothermic and ectothermic sharks. Journal of Experimental Biology, 206: 2845–2857.

Bernal, D., Donley, J. M., Shadwick, R. E., and Syme, D. A. 2005. Mammal-like muscles power swimming in cold-water shark. Nature, 437: 1349–1352.

Bernal, D., Sepulveda, C., Musyl, M., and Brill, R. 2009. The ecophysiology of swimming and movement patterns of tunas, billfishes, and large pelagic sharks. *In* Fish Locomotion: An Etho-Ecological Perspective, pp. 436–483. Ed. by P. Dominici and B.G. Kapoor. Science Publishers, Enfield, NH. 549 pp.

Block, B. A. 1986. Structure of the brain and eye heater tissue in marlins, sailfish, and spearfishes. Journal of Morphology, 190: 169–189.

Block, B. A., and Finnerty, J. R. 1994. Endothermy in fishes: a phylogenetic analysis of constraints, predispositions, and selection pressures. Environmental Biology of Fishes, 40: 283–302.

Bone, Q., and Chubb, A. D. 1983. The retial system of the locomotor muscles in the thresher shark. Journal of Marine Biology Association UK, 63: 239–241.

Brill, R. W. 1994. A review of temperature and oxygen tolerance studies of tunas, pertinent to fisheries oceanography, movement models, and stock assessments. Fisheries Oceanography, 3: 206–216.

Brill, R. W., Dewar, H., and Graham, J. B. 1994. Basic concepts relevant to heat transfer in fishes, and their use in measuring the physiological thermoregulatory abilities of tunas. Environmental Biology of Fishes, 40: 109–124.

Brill, R. W., and Lutcavage, M. E. 2001. Understanding environmental influences on movements and depth distributions of tunas and billfishes can significantly improve population assessments. American Fisheries Society Symposium, 25: 179–198.

Carey, F. G., and Teal, J. M. 1966. Heat conservation in tuna fish muscle. Proceedings of the National Academy of Sciences of the United States of America, 56: 1464–1469.

Carey, F. G., and Teal, J. M. 1969. Regulation of body temperature by the bluefin tuna. Journal of Comparative Biochemistry and Physiology, 28: 2015–2213.

Carey, F. G., Teal, J. M., Kanwisher, J. W., Lawson, K. D., and Becket, J. S. 1971. Warm-bodied fish. American Zoologist, 11: 135–143.

Carey, F. G., and Lawson, K. D. 1973. Temperature regulation in free-swimming bluefin tuna. Comparative Biochemistry and Physiology Part A Comparative Physiology, 44: 375–392.

Carey, F. G., and Robinson, B. H. 1981. Daily patterns in the activities of swordfish (*Xiphias Gladius*) observed by acoustic telemetry. Fishery Bulletin, 79: 277–292.

Carey, F. G. 1982. A brain heater in swordfish. Science, 216: 1327–1329.

Carey, F. G., Kanwisher, J. W., Brazier, O., Gabrielson, G., Casey, J. G., and Pratt, H. L. 1982. Temperature and activities of a white shark, *Carcharodon carcharias*. Copeia, 2: 254–260.

Carey, F. G., Casey, J. G., Pratt, H. L., Urquhart, D., and McCosker, J. E. 1985. Temperature, heat production and heat exchange in lamnid sharks. *In* Biology of the White Shark, pp. 92–108. Ed. by J. A. Seigel and C. C. Swift. Southern California Academy of Sciences, Los Angeles, CA. 150 pp.

Carey, F. G., and Gibson, Q. H. 1987. Blood flow in the muscle of free-swimming fish. Physiological Zoology, 60: 138–148.

Carey, F. G. 1990. Further acoustic telemetry observations of swordfish. *In* Planning the Future of Billfishes, pp. 103–132. Ed. by R.H. Stroud. National Coalition for Marine Preservation, Savannah, GA.

Dewar, H., Brill, R. W., and Olso, K. R. 1994. Secondary circulation of the vascular heat exchangers in skipjack tuna, *Katsuwonus pelamis*. Journal of Experimental Biology, 269: 566–570.

Dewar, H., Graham, J. B., and Brill, R. W. 1994b. Studies of tropical tuna swimming performance in a large water-tunnel II: thermoregulation. Journal of Experimental Biology, 192: 33–44.

Dewar, H., Prince, E. D., Musyl, M. K., Brill, R. W., Sepulveda, C. A., Luo, J., Foley, D. et al. 2011. Movements and behaviours of swordfish in the Atlantic and Pacific oceans examined using pop-up satellite archival tags. Fisheries Oceanography, 2: 219–241.

Dickson, K. A. 1994. Tunas as small as 207mm fork length can elevate muscle temperatures significantly above ambient water temperature. Journal of Experimental Biology, 190: 79–93.

Dickson, K. A. 1995. Unique adaptations of the metabolic biochemistry of tunas and billfishes for life in the pelagic environment. Environmental Biology of Fishes, 42: 65–97.

Dickson, K. A. 1996. Locomotor muscle of high-performance fishes: what do comparisons of tuna with ectothermic sister taxa reveal? Comparative Biochemistry and Physiology Part A, 113: 39–49.

Dickson, K. A., and Graham, J. B. 2004. Evolution and consequences of endothermy in fishes. Physiological and Biochemical Zoology, 77: 998–1018.

Dizon, A. E., and Brill, R. W. 1979a. Thermoregulation in yellowfin tuna, *Thunnus albacares*. Physiological Zoology, 52: 581–593.

Dizon, A. E., and Brill, R. W. 1979b. Thermoregulation in tunas. American Zoologist, 19: 249–265.

Domeier, M. L., Kiefer, D., Nasby-Lucas, N., Wagschal, A., and O'Brien, F. 2005. Tracking Pacific bluefin tuna (*Thunnus thynnus orientalis*) in the northeastern Pacific with an automated algorithm that estimates latitude by matching sea-surface temperature data from tags on fish. U.S. Fisheries Bulletin, 103: 292–306.

Donley, J. M., Shadwick, R. E., Sepulveda, C. A., and Syme, D. A. 2007. Thermal dependence of contractile properties of the aerobic locomotor muscle in the leopard shark and shortfin mako shark. Journal of Experimental Biology, 210: 1194–1203.

Donley, J. M., Sepulveda, C. A., Aalbers, S. A., McGillivray, D. G., Syme, D. A., and Bernal, D. 2012. Effects of temperature on power output and contraction kinetics in the locomotor muscle of the regionally endothermic common thresher shark (*Alopias vulpinus*). Fish Physiology and Biochemistry, 38: 1507–1519.

Fritsches, K. A., Brill, R. W., and Warrant, E. J. 2005. Warm eyes provide superior vision in swordfishes. Current Biology, 15: 55–58.

Graham, J. B. 1974. Heat exchange in the yellowfin tuna, *Thunnus albacares*, and skipjack tuna, *Katsuwonus pelamis*, and the adaptive significance of elevated body temperatures. Fishery Bulletin, 73: 219–229.

Graham, J. B., Koehrn, F. J., and Dickson, K. A. 1983. Distribution and relative proportions of red muscle in scombrid fishes: consequences of body size and relationships to locomotion and endothermy. Canadian Journal of Zoology, 61: 2087–2096.

Holland, K., Brill, R., Chang, R., Sibert, J., and Fournier, D. 1992. Physiological and behavioural thermoregulation in bigeye tuna (*Thunnus obesus*). Nature, 358: 410–412.

Holland, K. N., and Sibert, J. R. 1994. Physiological thermoregulation in bigeye tuna, *Thunnus obesus*. Environmental Biology of Fishes, 40: 319–327.

Johnston, I. A. 1981. Structure and function of fish muscles. *In* Vertebrate Locomotion, pp. 71–113. Ed. by M. H. Day. Symposia of the Zoological Society of London, London.

Johnston, I. A., and Brill, R. W. 1984. Thermal dependence of contractile properties of singled skinned muscle fibers from Antarctic and various warm water fishes including skipjack tuna (*Katsuwonus pelamis*) and kawakawa (*Euthynnus affinis*). Journal of Comparative Physiology Part B, 155: 63–70.

Jones, D. R., and Randall, D. J. 1978. The respiratory and circulatory systems during exercise. Fish Physiology, 7: 425–501.

Kitagawa, T., and Kimura, S. 2004. An alternative heat-budget model relevant to heat transfer in fishes and its practical use for detecting their physiological thermoregulation. Zoological Society of Japan, 23: 1065–1071.

Korsmeyer, K. E., and Dewar, H. 2001. Tuna metabolism and energetics. *In* Tuna: Physiology, Ecology and Evolution, Fish Physiology, vol. 19, pp. 35–78. Ed. by B. A. Block and E. D. Stevens. Academic Press, San Diego. 468 pp.

Lowe, T., Brill, R., and Cousins, K. 2001. Blood O_2-binding characteristics of bigeye tuna (*Thunnus obesus*), a high-energy demand teleost that is tolerant of low ambient O_2. Marine Biology, 136: 1087–1098.

Malte, H., Larsen, C., Musyl, M., and Brill, R. 2009. Differential heating and cooling rates in bigeye tuna (*Thunnus obesus* Lowe): a model of non-steady heat exchange. Journal of Experimental Biology, 210: 2618–2626.

Musyl, M. K., Brill, R. W., Boggs, C. H., Curran, D. S., Kazama, T. K., and Seki, M. P. 2003. Vertical movements of bigeye tuna (*Thunnus obesus*) associated with islands, buoys, and seamounts near the main Hawaiian Islands from archival tagging data. Fisheries Oceanography, 12: 1–18.

Musyl, M. K., McNaughton, L. M., Swimmer, J. Y., and Brill, R. W. 2004. Convergent evolution of vertical movement behaviour in swordfish, bigeye tuna, and bigeye thresher sharks. Pelagic Fisheries Research Program, 9: 1–4.

Nakano, H., Matsunaga, H., Okamoto, H., and Okazaki, M. 2003. Acoustic tracking of bigeye thresher sharks *Alopias superciliosus* in the eastern Pacific Ocean. Marine Ecology Progress Series, 265: 255–261.

Neill, W. H., and Stevens, E. D. 1974. Thermal inertia versus thermoregulation in "warm" turtles and tunas. Science, 184: 1008–1010.

Neill, W. H., Chang, R. K. C., and Dizon, A. E. 1976. Magnitude and ecological implications of thermal inertia in skipjack tuna, *Katsuwonus pelamis* (Linnaeus). Environmental Biology of Fishes, 1: 61–80.

Patterson, J. C., Sepulveda, C. A., and Bernal, D. 2011. The vascular morphology and in vivo muscle temperatures of thresher sharks (Alopiidae). Journal of Morphology, 272: 1353–1364.

Schaefer, K. M., Fuller, D. W., and Block, B. A. 2009. Vertical movements and habitat utilization of skipjack (*Katsuwonus pelamis*), yellowfin (*Thunnus albacares*), and bigeye (*Thunnus obesus*) tunas in the equatorial Eastern Pacific Ocean, ascertained through archival tag data. *In*: Tagging and Tracking of Marine Animals with Electronic Devices, pp. 121–144. Ed. by J. J. Neilson, H. Arrizabalaga, N. Fragoso, A. Hobday, M. Lutcavage, and J. Sibert. Springer, New York. 443 pp.

Sepulveda, C. A., Knight, A., Nasby-Lucas, N., and Domeier, M. L. 2010. Fine-scale movements of the swordfish, *Xiphias Gladius*, in the Southern California Bight. Fisheries Oceanography, 19: 279–289.

Sepulveda, C. A., Aalbers, S. A., and Heberer, C. 2014. Testing modified deep-set buoy gear to minimize bycatch and increase swordfish selectivity. BREP, 1: 27–32.

Stevens, E. E., and Randall, D. J. 1967. Changes of gas concentrations in blood and water during moderate swimming activity in rainbow trout. Journal of Experimental Biology, 46: 329–337.

Stevens, E. D., Lam, H. M., and Kendall, J. 1974. Vascular anatomy of the counter-current heat exchanger of skipjack tuna. Journal of Experimental Biology, 61: 145–153.

Stillwell, C. E., and Kohler, N. E. 1982. Food, feeding habits, and estimates of daily ration of the shortfin mako (*Isurus oxyrinchus*) in the Northwestern Atlantic. Canadian Journal of Fisheries and Aquatic Sciences, 39: 407–414.

Syme, D. A., and Shadwick, R. E. 2011. Red muscle function in stiff-bodied swimmers: there and almost back again. Philosophical Transactions of the Royal Society B, 366: 1507–1515.

Takahashi, M., Okamura, H., Yokawa, K., and Okazaki, M. 2003. Swimming behaviour and migration of swordfish recorded by an archival tag. Marine and Freshwater Research, 54: 527–534.

Ward, P., Porter, J. M., and Elscot, S. 2000. Broadbill swordfish: status of established fisheries and lessons for developing fisheries. Fish and Fisheries, 1: 317–336.

Watanabe, Y. Y., Goldman, K. J., Caselle, J. E., Chapman, D. D., and Papastamatiou, Y. P. 2015. Comparative analyses of animal-tracking data reveal ecological significance of endothermy in fishes. Proceedings of the National Academy of Sciences of the United States of America, 112: 6104–6109.

Wegner, N. C., Sepulveda, C. A., Bull, K. B., and Graham, J. B. 2010. Gill morphometrics in relation to gas transfer and ram ventilation in high-energy demand teleosts: scombrids and billfishes. Journal of Morphology, 271: 36–49.

Young, B., Heath, J. W., Stevens, A., Lowe, J. S., Wheater, P. R., and Burkitt, H. G. 2000. Wheater's Functional Histology: A Text and Colour Atlas, 6th edn, Churchill Livingstone, Edinburgh. 464 pp.

Handling editor: Erika J. Eliason